Chapter 3

X-RAY STANDING WAVEFIELD IN COMPLEX CRYSTAL STRUCTURES

Victor Kohn

Russian Research Center "Kurchatov Institute,"
123182, Moscow, Russia

The theory of the secondary radiation yield generated by the X-ray standing wave field from layered crystals based on an analytical solution of the Takagi equations for a single layer is presented. Each layer is described by its own set of structural parameters which are constant within the layer. Both Bragg and Laue cases are discussed within the same approach. The secondary radiation is considered to originate through the photoelectron absorption with the exponential yield probability function. A computational algorithm based on recurrent equations is described.

3.1. Introduction

The X-ray standing wavefield (XSW) technique is based on measuring the secondary radiation yield (SRY) due to incoherent scattering of X-rays under the condition of the two-beam dynamical diffraction in nearly perfect crystals. Various channels of incoherent scattering may be considered, each of them yielding its own unique structural or physical information. In this section, we will deal with the SRY originating through the photoelectric absorption, i.e. fluorescence and photoelectron emission. The probability of the atomic excitation and the emission of a photoelectron or a fluorescent quantum is proportional to the total E-field, which is a coherent superposition of the transmitted and reflected plane waves at atomic position (dipole approximation).

There are two physical processes that define the angular dependence of the XSW yield. First is the extinction effect, which is characterized by the extinction length L_{ex}. We define L_{ex} as a depth at which the XSW

intensity is reduced by e times at the angular position of the center of the Bragg peak. The second process is the absorption of the secondary radiation on its way from the emitting atom to the surface of a crystal. It can be described by a yield probability function (YPF) first introduced in Ref. 1 as a probability of the secondary radiation originated at the depth z to escape the crystal. For fluorescent photons, the YPF is an exponential function $\exp(-\mu_{yi}z)$ with the characteristic length $L_{yi} = \mu_{yi}^{-1}$, where μ_{yi} is a linear absorption coefficient. For photoelectrons, in general, the YPF has a more complex form and it was studied in Ref. 2 by using Monte Carlo computer simulation. It was shown[3] that, at least for the integrated over energy photoelectron yield, the YPF can be also approximated by an exponential function with the characteristic length $L_{yi} \ll L_{ex}$.

The relationship between L_{ex} and L_{yi} determines the shape of the XSW yield curve. If $L_{yi} \gg L_{ex}$, the situation that is typical for the fluorescence originating from the bulk atoms, the extinction effect dominates and the structural information is almost entirely lost. For fluorescence originating from an atomic layer on the surface $L_{yi} \ll L_{ex}$ and the XSW curve contains unique structural information about specific location of absorbed atoms (see Ref. 4 and Chapters 20 and 21 on applications of XSW in surface science). This situation is adequately described by the dynamical theory in perfect crystals (e.g. Chapter 2).

It was discovered in the early years of the development of the XSW method that if crystal contains a surface layer with a structure different from the bulk, the yield of a secondary radiation with $L_{yi} \ll L_{ex}$ is extremely sensitive to the structure of this layer. This layer may be a layer of the same crystal artificially altered by a special treatment (e.g. ion implantation, diffusion, polishing, and laser annealing) or it may be an epitaxial film of a different material. In general, since the surface layer alters the XSW field the XSW yield from such crystals cannot be described by simple equations derived for perfect crystals.

A theoretical approach to this problem was proposed in Ref. 1. It was based on a solution of Takagi equations to calculate the local electric field inside the crystal and on taking into account the YPF for a particular SRY and integrating it over the thickness of the sample. For a crystal with structural parameters varied as a function of depth z, the Takagi equations can be solved only numerically. In many cases, however, the sample can be approximated as a crystal consisting of several layers with structural parameters that are constant with the thickness of an individual layer. Then, the recurrent relations based on an analytical solution for a single layer can be utilized to solve the problem numerically. Such an approach

was used for both the Bragg[3] and for the Laue[5] cases to analyze specific experimental results and was later summarized in the most recent form in Ref. 6.

The chapter is organized as follows. In the Sec. 3.2., the analytical solution for the local reflection and transmission amplitudes is derived for a single crystalline layer. Then, the YPF is introduced and the integration over the thickness of the sample is performed. It will be followed by the description of a numerical algorithm. The set of parameters required to compute the XSW yield from a multilayer crystalline structure will be presented and discussed, followed by a computational example and summary.

3.2. Solution for One Crystal Layer

Let us consider a single crystal of a lamina-like shape and a case of the two-beam diffraction on a reciprocal lattice vector **h**. The solution of the Maxwell's equation can be sought in the form

$$\mathbf{E}(\mathbf{r},\omega) = \exp(i\mathbf{k}_0\mathbf{r})[\mathbf{e}_0 E_0(z) + \mathbf{e}_h E_h(z)\exp(i\mathbf{hr})], \tag{3.1}$$

where $\mathbf{e}_0$, $\mathbf{e}_h$ are the unit polarization vectors, $\mathbf{k}_0$ is the wave-vector of the incident plane wave in the air, $|\mathbf{k}_0| = K$ where $K = \omega/c = 2\pi/\lambda$, c is the speed of light, and λ is the wavelength of X-rays, z is the depth inside the crystal. The complex functions $E_{0,h}(z)$ are slowly varying in space compared to the exponential $\exp(i\mathbf{hr})$. We assume the incident wave to be a plane-polarized wave, which is a valid assumption for synchrotron radiation. In the case of a nonpolarized radiation, one has to consider two standard polarization states separately and average intensity over polarizations states.

The integration of the Maxwell's equation over unit cell allows us to write the set of two equations for $E_0(z)$, and $E_h(z)$:

$$\begin{aligned} 2\gamma_0 \frac{dE_0}{dz} &= iK\left\{\chi_0 E_0 + C\chi_{\overline{h}}\exp(i\varphi - W)E_h\right\}, \\ 2\gamma_h \frac{dE_h}{dz} &= iK\left\{[\chi_0 - \alpha]E_h + C\chi_h \exp(-i\varphi - W)E_0\right\}, \end{aligned} \tag{3.2}$$

where $\gamma_0 = k_{0z}/K$, and $\gamma_h = k_{hz}/K$ are the geometrical parameters, $\alpha = [\mathbf{k}_h^2 - \mathbf{k}_0^2]/K^2$ is the parameter of deviation from the Bragg condition, $\mathbf{k}_h = \mathbf{k}_0 + \mathbf{h}$ is the wave vector of the diffracted wave, $C = (\mathbf{e}_0\mathbf{e}_h)$ is the polarization factor, and $\varphi(z) = \mathbf{hu}(z)$ is an additional phase due to a

mean displacement of atoms from their equilibrium positions by a vector **u**. The quantities χ_0, χ_h, and $\chi_{\overline{h}}$ are the Fourier coefficients of the crystal susceptibility with the reciprocal lattice vectors 0, **h**, $-$**h**. Finally, the factor $\exp[-W(z)]$ describes dephasing of the scattered wave due to random displacements of atoms from their mean value at depth z. This factor was introduced for the first time in Ref. 1 and called the static Debye–Waller factor on analogy with a well-known thermal Debye–Waller factor, which is incorporated into the crystal susceptibility.

The boundary conditions for Eq. (3.2) depend on a sign of the geometrical parameter γ_h. In the Laue case, $\gamma_h > 0$ and the diffracted beam is escaping the crystal through the back surface and absent at the entrance surface; therefore, we have $E_0(0) = 1$ and $E_h(0) = 0$. Here and later on we assume that the entrance surface is at $z = 0$ and the incident intensity is normalized to unity. In the Bragg case, $\gamma_h < 0$ and the diffracted beam is escaping from the entrance surface and absent at the back surface, so we have $E_0(0) = 1$ and $E_h(d) = 0$, where d is the thickness of the crystal plate.

3.2.1. *Local reflection amplitude*

We will consider the Bragg and the Laue cases simultaneously. The boundary conditions do not allow us to move from the entrance surface step by step. It is convenient to divide a problem into two parts and to introduce first a local reflection amplitude as the ratio

$$R(z) = \frac{E_h(z)}{E_0(z)} \frac{\exp[i\varphi(z)]}{Y\,\beta^{1/2}}. \tag{3.3}$$

This variable obeys the nonlinear equation which can be derived from the set of Eq. (3.2)

$$\frac{dR(z)}{dz} = -\frac{2is}{L_{ex}}[y - y_\varphi(z) + iy_0]R(z) + \frac{iC_1}{L_{ex}}[s + R^2(z)], \tag{3.4}$$

where the variables are introduced: $C_1 = C(1 - ip)\exp(-W)$,

$$L_{ex} = \frac{\lambda\gamma_0}{\pi\beta^{1/2}X'}, \quad X = (\chi_h\chi_{\overline{h}})^{1/2} = X' + iX'' = X'(1 - ip), \tag{3.5}$$

$$Y = \left(\frac{\chi_h}{\chi_{\overline{h}}}\right)^{1/2} = |Y|\exp(i\Phi_Y), \quad y = -\frac{[\alpha\beta - s\chi_0'(1 + s\beta)]}{2\beta^{1/2}X'}, \tag{3.6}$$

$$y_0 = \frac{s\chi_0''(1 + s\beta)}{2\beta^{1/2}X'}, \quad y_\varphi(z) = s\frac{L_{ex}}{2}\frac{d\varphi(z)}{dz}, \quad \beta = \frac{\gamma_0}{|\gamma_h|}. \tag{3.7}$$

Here we use notations a' and a'' for the real and imaginary parts of a complex value a. The parameter s is equal to 1 for the Bragg case and -1 for the Laue case. The boundary conditions for the local reflection amplitude are as follows: $R(0) = 0$ in the Laue case and $R(d) = 0$ in the Bragg case.

There are two ways of changing the parameter of deviation from the Bragg condition α. The first one is to change the angle of incidence θ of the X-ray beam by $\Delta\theta$ while keeping the energy constant. In this case we have

$$y = C_{y\theta}\,\Delta\theta, \quad y_\varphi(z) = C_{y\theta}\,\Delta\theta_B(z), \quad C_{y\theta} = \pi\frac{L_{ex}}{\lambda|\gamma_h|}\sin 2\theta_B, \tag{3.8}$$

where θ_B is the Bragg angle in a perfect crystal while $\Delta\theta_B(z)$ is a local shift of the Bragg angle at the depth z due to distortions of the crystal lattice. The angle $\Delta\theta$ is positive if $\theta > \theta_B$. The second way is to change the energy of X-ray photons, keeping constant the direction of the beam. In this case

$$y = C_{y\omega}\,\Delta(\hbar\omega), \quad y_\varphi(z) = C_{y\omega}\,\Delta(\hbar\omega_B(z)), \quad C_{y\omega} = \frac{L_{ex}}{\hbar c|\gamma_h|}\sin^2\theta_B \tag{3.9}$$

where $\hbar = h/2\pi$, h is the Planck constant, $\hbar\omega_B$ is the Bragg energy of X-ray photons. Parameters $\Delta\theta_B(z)$ and $\Delta(\hbar\omega_B(z))$ describe a local shift of the Bragg angle or energy at depth z due to distortions. The origin of the y-axis corresponds to the center of the diffraction peak for a perfect crystal. The $\Delta\theta$-dependence is common for experiments in a nondispersive arrangement, e.g. with laboratory X-ray sources. The $\Delta(\hbar\omega)$-dependence is often used in experiments with synchrotron radiation when the energy is scanned by the upstream monochromator, e.g. at near backscattering conditions with $\theta_B \approx \pi/2$. Note that the parameter y_0 can also be expressed through the dimensionless variables $y_0 = (s\mu_0/4\gamma_0)L_{ex}(1 + s\beta)$ where $\mu_0 = 2\pi\chi_0''/\lambda$ is a linear absorption coefficient.

The method based on a direct numerical solution of the differential equation (3.4) was proposed in Ref. 7 and discussed in Ref. 8. However, such an approach has a disadvantage for a crystal containing thick layers with approximately constant parameters and a large difference in parameters between the layers. Indeed, to have sufficient accuracy in numerical processing of Eq. (3.4), a very small step Δz is required over the total thickness of the layer even if parameters within this layer are almost constant. It is more convenient to consider a crystal as a set of layers with the parameters that are constant within each layer and can be changed only at the layers boundaries. Equation (3.4) for a layer with the constant parameters y_φ has an analytical solution. Here we present the general

solution[6] that is valid for both the Bragg and the Laue cases. In addition, we assume that the boundary conditions for each layer does not contain zero amplitudes, i.e. the amplitudes $R(0)$ in the Laue case and $R(d)$ in the Bragg case are finite and known, where d is now the thickness of the layer, not the thickness of a sample. We omit the derivation and present the solution in the form

$$R(z) = \frac{x_1 - x_2 B \exp(-is\sigma z)}{F_d(z)}, \quad F_d(z) = 1 - B\exp(-is\sigma z), \tag{3.10}$$

where

$$x_{1,2} = -\frac{s}{C_1}[-a \pm \sqrt{a^2 - sC_1^2}], \quad \sigma = \frac{2}{L_{ex}}\sqrt{a^2 - sC_1^2}, \tag{3.11}$$

$$a = y - y_\varphi + iy_0, \quad B = \frac{(x_1 - R(z_b))}{(x_2 - R(z_b))}\exp(i\sigma z_b). \tag{3.12}$$

Here and later on it is assumed that square roots have positive imaginary parts. One can verify the solution by the direct substitution. Equations (3.10) to (3.12) allow one to derive the recurrent relation for the reflection amplitude at the exit surface $z = z_e$ from the known value at the entrance surface $z = z_b$.

$$R(z_e) = \frac{(x_1 - x_2)R(z_b) + x_2[x_1 - R(z_b)][\exp(i\sigma d) - 1]}{x_1 - x_2 + [x_1 - R(z_b)][\exp(i\sigma d) - 1]}. \tag{3.13}$$

The parameters z_e and z_b are $z_e = d$ and $z_b = 0$ in the Laue case and $z_e = 0$ and $z_b = d$ in the Bragg case.

The accurate solution presented above allows us to easily consider analytical kinematical approximations. If $d \to 0$, we obtain the same expression, which can be obtained directly from Eq. (3.4) if one takes the right-hand side of the equation at the boundary and replace a derivative by $[R(z_e) - R(z_b)]/(-sd)$. In a pure kinematical case, when $|R(z)| \ll 1$ and $|aR(z)| \ll 1$, we have a simple expression $R(z_e) = R(z_b) - idC_1/L_{ex}$ meaning that the reflection amplitude linearly increases with thickness independently on the parameter of deviation from the Bragg condition. Another kinematical approximation can be obtained for a large deviation from the Bragg condition, $|a| \gg |C_1|$. Under this condition in the Bragg case we have $\sqrt{a^2 - sC_1^2} \approx a$. Then $x_1 \approx 0$, $x_2 \approx 2a/C_1$, $|x_2| \gg 1$, $\sigma d = \Phi = 2ad/L_{ex}$, and we obtain from Eq. (3.13) that $R(z_e) = R(z_b)\exp(i\Phi)$. This means that the layer changes the phase of the reflection amplitude which

may have a large modulus due to reflection at the substrate. The layer does not influence practically the modulus of the reflection amplitude. As for the phase, it can be measured by means of XSW.

3.2.2. *Local transmission amplitude*

Taking into account the definition (3.3), we can write a straightforward solution of the first Takagi equation as follows

$$E_0(z) = \exp\left\{ i\frac{\pi\chi_0}{\lambda\gamma_0} z - i\frac{C_1}{L_{ex}} \int_0^z dz'\, R(z') \right\} E_0(0) = T(z)E_0(0). \quad (3.14)$$

The solution may be used for a numerical calculation, however, again with a disadvantage owing to the integral. For a constant parameter y_φ the function $R(z)$ has the analytical expression (3.10) and the integral can be calculated analytically by means of a table integral. The result looks as follows

$$T(z) = \exp(\frac{i}{2}Gz)\frac{F_d(z)}{F_d(0)}, \quad (3.15)$$

where

$$G = G' + iM = 2\frac{\pi\chi_0}{\lambda\gamma_0} - 2\frac{C_1}{L_{ex}}x_1, \quad M = \frac{\mu_0(1 - s\beta)}{2\gamma_0} + s\sigma'' \quad (3.16)$$

Here $M = G''$ and the values x_1 and $F_d(z)$ are defined above. As one can observe, the recurrent relation for the intensity of the transmitted wave has a simple form. However, to use this expression, one needs to know the value $R(z_b)$ for this layer. Therefore, this recurrent relation may be used only after the recurrent relation (3.13) is applied.

3.3. Secondary Radiation Yield

We consider the XSW techniques based on measuring the intensity of the secondary radiation scattered via photoelectron emission or fluorescence. This radiation involves many spherical waves originating from individual atoms. If a SRY detector counts all electrons or photons that reach the surface, the YPF must be averaged over the surface. Then, the averaged YPF $P_{yi}(z)$ depends only on the z-coordinate, which the distance between atoms emitting radiation and the surface. As we discussed in Sec. 1, we consider the YPF in the form of an exponential function $P_{yi}(z) = \exp(-\mu_{yi}z)$.

Below we assume that the SRY detector collects radiation from the entrance surface. For the radiation collected from the exit surface we may formally consider a negative value of μ_{yi}. Both types of secondary radiation, fluorescence and photoelectrons, are generated via a resonant interaction of x rays with atoms. Within a dipole approximation the intensity of the SRY emitted from atom is proportional to the intensity of the X-ray field at atomic position and the size of atom is assumed to be negligibly small. To take into account the size of atom we need to add a quadrupole term of the multipole expansion.[8] Thermal vibrations and static atomic displacements from equilibrium positions are accounted for by the thermal and static Debye–Waller factors.

Consider again a layered crystal. Each layer is uniform, i.e. the structural parameters are constant within the thickness of the layer, however, they may differ for different layers. Then, the total yield of secondary radiation I_{SR} is a sum over all layers

$$I_{SR} = \sum_{n=1}^{N} Z_{n-1}\, I_{SR}^{(n)}, \quad Z_n = |E_0(z_n)|^2 P_{yi}(z_n), \tag{3.17}$$

where $I_{SR}^{(n)}$ is a contribution of the layer with the back boundary at z_n ($z_0 = 0$). The thickness of the n-th layer is $d_n = z_n - z_{n-1}$. Using solution (3.10), we write expression for $I_{SR}^{(n)}$ in terms of the local reflection amplitude

$$I_{SR}^{(n)} = \chi''_{0a} \int_0^d dz'\, P_{yi}(z')|T(z')|^2 \big[1 + |R(z')|^2 |Y\,|^2 \beta + 2\mathrm{Re}\big\{R(z') \times Y\beta^{1/2} C(\chi''_{ha}/\chi''_{0a}) \exp[-i\varphi(z') + i\varphi_a(z')]\big\} \exp[-W_a]\big] \tag{3.18}$$

where the index a indicates that the yield is calculated only for atoms contributing into the SRY, $\varphi_a(z) = \mathbf{hu}_a(z)$. All the parameters must be taken for the n-th layer.

To move further we accept a reasonable assumption that the difference $\varphi(z) - \varphi_a(z) = \Delta\varphi_a$ does not depend on z. If the emitting atoms occupy crystal lattice nodes, then $\Delta\varphi_a = 0$. In a general case of atoms occupying position defined by the vector $\mathbf{u}_a$ within the unit cell (e.g. impurity atoms in interstitial positions) this parameter is nonzero and the integral can be calculated analytically. The result can be written as:

$$I_{SR}^{(n)} = \frac{d_n \chi''_{0a}}{|1 - B\,|^2} \left[A_1 \Psi_1 + A_2 \Psi_2 - \mathrm{Re}(A_3 \Psi_3)\right] \tag{3.19}$$

where B is determined by Eq. (3.12) and

$$A_1 = 1 + |x_1|^2 C_r + \mathrm{Re}(C_i x_1), \tag{3.20}$$

$$A_2 = |B\,|^2 [1 + |x_2|^2 C_r + \mathrm{Re}(C_i x_2)], \tag{3.21}$$

$$A_3 = B(2[1 + x_1^* x_2 C_r] + (C_i x_1)^* + C_i x_2) \tag{3.22}$$

$$\Psi_k = [1 - \exp(-a_k)]\,/\,a_k, \quad k = 1, 2, 3, \tag{3.23}$$

Here we introduced the following abbreviations

$$a_1 = (M + \mu_{yi})\,d, \quad a_2 = a_1 - 2s\sigma'' d, \quad a_3 = a_1 + is\sigma d, \tag{3.24}$$

$$C_r = |Y\,|^2 \beta, \quad C_i = 2CY\beta^{1/2} f_c \exp(i\varphi_c), \tag{3.25}$$

$$f_c = (|\chi''_{\bar{h}a}|/\chi''_{0a}) \exp(-W_a), \quad \varphi_c = \Delta\varphi_a - \arg(\chi''_{ha}) \tag{3.26}$$

The parameters f_c and $P_c = -\varphi_c/2\pi = d_c/d_{hkl}$ are the coherent fraction and coherent position of atoms emitting secondary radiation, in a full analogy with the same parameters introduced in the first chapters of this book. Hereafter, d_{hkl} is a distance between the reflecting atomic planes and d_c is a displacement of atoms from the origin of the unit cell along the reciprocal lattice vector. We note again that the Eq. (3.19) is valid for both the Bragg and the Laue cases with the difference only in the sign of the symbol s.

3.4. Method of the Computer Simulation

A general solution for the XSW yield from a single layer was used for developing computer program *SWAN* which is elaborated by using programming language Java 1.4.2 and now available on the web.[9] Below, computing algorithm and the main features of the program are described. We assume that the crystal contains N layers. Each layer can be characterized by its own crystal structure and atomic composition. In particular, extinction length defined by the value of X' can be different for different layers leading to different scaling coefficients in Eqs. (3.8) and (3.9). To overcome this problem, the same value of extinction length $L_{ex}^{(0)} = \lambda\gamma_0(\pi\beta^{1/2}X'_0)^{-1}$, where X'_0 is a reference value for X', was introduced for all layers. Simultaneously, the static Debye–Waller factor for each layer was replaced by the parameter $f_{sc} = \exp(-W)(X'/X'_0)$, which can be called the scattering power of the layer. Such a replacement does not change Takagi equations and does not influence the results.

One may distinguish 11 parameters which characterize the layer completely, namely: (1) d — thickness of the layer; (2) $\Delta\theta_B$ or $\Delta(\hbar\omega_B)$ — shift of the Bragg angle or the Bragg energy; (3) f_{sc} — scattering power; (4) μ_0 — linear absorption coefficient of incident x rays; (5) μ_{yi} — absorption coefficient of a secondary radiation, (6) $p = -X''/X'$ as defined by Eq. (3.5); (7) $|Y|$ as defined by Eq. (3.6); (8) $\arg(Y)$ as defined by Eq. (3.6); (9) f_c is a coherent fraction; (10) φ_c is a phase corresponding to a relative coherent position; and (11) χ''_{0a} is a power of the SRY. The latter parameter allows one to take into account relative differences in the amount of atoms in different layers contributing to the same SRY. For a layer not contributing to SRY, this parameter is zero.

If the parameter Y has different values in the neighboring layers, the values of the product YR must be the same at both sides of the boundary between these layers. Therefore we must apply the transition condition as $R_n = R_{n\pm1}Y_{n\pm1}/Y_n$.

In the Bragg case the local reflection amplitude vanishes at the back side of the sample, i.e. $R(t) = 0$ where $t = z_N$ is a thickness of the sample. The measurable quantity is the reflectivity P_R defined by $P_R = |Y\,R(0)|^2$. Therefore, at first, we have to use the recurrent relation (3.13) N times from the back to the front surface of the crystal. Only after that we can calculate the secondary radiation yield I_{SR} by means of summation in Eq. (3.17), taking into account Eq. (3.19) and recurrent relation for coefficients Z_n as

$$Z_0 = 1, \quad Z_{n+1} = Z_n\,|T_n(d_n)|^2 \exp\big(-\mu_{yi}^{(n)} d_n\big) \tag{3.27}$$

The transmissivity P_T can be calculated using the same value as

$$P_T = Z_N \exp\left(\sum_{n=1}^{N} \mu_{yi}^{(n)} d_n\right) \tag{3.28}$$

In the Laue case $R(0) = 0$, and we should proceed in the opposite direction applying recurrent relation from the front to the back surface. In this case the reflectivity is not determined completely by the local reflection amplitude due to absorption and we have $P_R = |Y\,R(t)|^2 P_T$. The case of the secondary radiation escaping the crystal from the back surface can be calculated within the same method using the negative value of μ_{yi}. The normalization of the SRY curve to the unity background can be performed numerically.

So far we considered the incident beam as monochromatic and perfectly collimated. One can distinguish two experimental arrangements. In the first

one the angular dependence of the SRY is measured by rotating sample through the Bragg reflection. The incident beam is conditioned by using a crystal collimator. The energy spread of the incident beam is determined by the natural width of a characteristic line when using laboratory sources or by the properties of the upstream monochromator when using synchrotron radiation. In a typical XSW setup, a sample and monochromator (or, postmonochromator) crystals are arranged in a nondispersive $(n, -n)$ setup. Then, the parameter X' of the monochromator is equal or close to X_0' and a well-known formula can be used for convolution:

$$I_c(y) = \frac{1}{S} \sum_j \int dy_1 \, P_R^{(m)}(j, y_1) \, I\,(j, y + y_1[\beta_m \beta]^{1/2}), \tag{3.29}$$

$$S = \sum_j \int dy_1 \, P_R^{(m)}(j, y_1). \tag{3.30}$$

Here β_m is an asymmetry factor for a monochromator crystal and j is an index of polarization. A notation $I(j, y)$ is used for any of the functions $P_R(j, y)$, $P_T(j, y)$, and $I_{SR}(j, y)$.

The second technique is often utilized when using SR source and based on scanning the energy of the incident beam by rotating the monochromator while keeping the angle of incidence fixed. Therefore, the energy dependence of the SRY is measured. In particular, this technique is standard for the near backscattering geometry. The energy spread of the incident beam is determined by the properties of the monochromator setup and the properties of a SR source. It is a common practice to approximate it by a Gaussian function. Then, in the y-scale we have

$$I_c(y) = (\sigma_y \sqrt{\pi})^{-1} \int dy_1 \, \exp(-y_1^2/\sigma_y^2) \, I\,(j, y + y_1) \tag{3.31}$$

where σ_y is used as a variable fitting parameter. Convolution with the Gaussian function can also be useful in the first case to account for some mosaicity.

Many of the 11 parameters describing each layer are usually very well known or can be calculated based on the knowledge of a preparation procedure, sample history, and the results of independent measurements by using complementary techniques. Other parameters have to be determined by fitting. The list of fitting parameters usually includes the thickness of the layer d, the shift of the Bragg angle $\Delta\theta_B$ or energy $\Delta(\hbar\omega_B)$, and the static Debye–Waller factor $\exp(-W)$. Fitting is performed by minimizing

the function

$$\chi^2 = \sum_i [I_c(\theta_i) - KI_{ex}(\theta_i)]^2, \tag{3.32}$$

where $I_{ex}(\theta_i)$ is the experimental data and $I_c(\theta_i)$ is the theoretical value calculated for the same data points. If experimental data are normalized, the scaling factor $K = 1$, otherwise the K value is determined for each combination of fitting parameters by using a well-known solution $K = \left(\sum_i I_{ex}^2(\theta_i)\right)^{-1} \sum_i I_c(\theta_i) I_{ex}(\theta_i)$.

3.4.1. *Example: InGaP/GaAs(111)*

As an example, consider $In_{0.5}Ga_{0.5}P$ film grown by the liquid phase epitaxy on $GaAs(111)$ surface. The polarity of the $GaAs$ substrate and the film is known and fixed such that the Ga atoms in the substrate and the In and Ga atoms in the film occupy top half of the (111) double layer. We are interested in the fluorescence yield from the In and P atoms from the film excited by the (111) Bragg reflection.[10] Both the substrate and the layer materials belong to a zincblend structure with four Ga atoms in the substrate and two In atoms and two Ga atoms in the film occupy the $(0,0,0;0,1/2,1/2;1/2,0,1/2;1/2,1/2,0)$ fcc sublattice while four As atoms in the substrate and four P atoms in the film occupy the $fcc + (1/4,1/4,1/4)$ sites. Then, the geometrical structure factors for In atoms $S_{In} = 1$ and for P atoms $S_P = i$ and, accordingly, $\varphi_c^{In} = 0$ and $\varphi_c^P = -\pi/2$. The X-ray reflectivity curve from the sample is shown on the bottom panel of Fig. 3.1, and the In-L and the P-K fluorescence yields from the film are on the top panels. Striking difference in the shape of the XSW curves for the In and P atoms is due to the difference by $\pi/2$ in the phases of their structure factors. The reflectivity and the fluorescence data were fitted by using the layer thickness, the difference in the Bragg angles for the substrate and the layer and the static DW factor as fitting parameters. It was assumed that the static DW factor for both In and P sublattices are the same and equal to the static DW factor of the layer as a whole. The best fit within a single layer model is shown by a thin line. The quality of the fit can be improved if a thin layer with different lattice constant is introduced at the interface (thick solid line, see Ref. 6 for details). The remaining discrepancy in the fit of the P fluorescence data may be due to the secondary excitations not accounted for in this model. These results (i) proved that the XSW fluorescence bears direct information about the phases of the

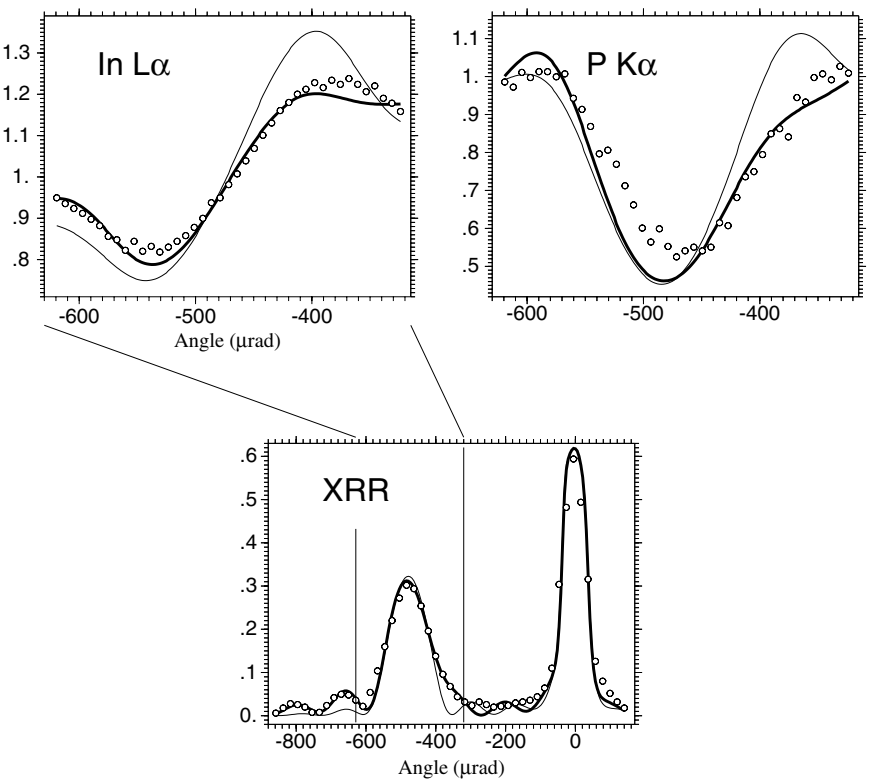

Fig. 3.1. X-ray reflectivity (bottom panel) and fluorescence yield from the In (top left panel) and P (top right panel) atoms from the $In_{0.5}Ga_{0.5}P$ films grown by liquid phase epitaxy on GaAs(111) substrate. The fluorescence data are in the angular range of the Bragg peak from the film. The best fit within a single layer model (thin line) and the model with a thin interface layer (thick line) are shown. The shape of the fluorescence curve is determined by the phase of the structure factor of the corresponding sublattice. (From Refs. 6 and 10).

structure factors of the individual sublattices in multicomponent films and (ii) demonstrated that a more detailed information about the depth profile can be obtained when the X-ray reflectivity is assisted by a phase sensitive XSW data.

3.5. Brief Historical Overview and Summary

The first version of the computer program based on the theory presented in this section was developed by the author in 1980s stimulated by

the pioneering experiments performed by Russian scientists in which photoelectron emission excited by the XSW from perfect crystals was studied.[11] Potential applications of this technique as a tool to study the structure of surface layers had been quickly realized and first experiments on crystals with amorphous layers,[12] ion implanted layers,[13] and epitaxial films[3] were performed. In the 1990s, the author continued developing his program motivated by the new experimental results and working in close collaboration with the researches from the laboratory of Michael Kovalchuk, Institute of Crystallography, Russian Academy of Science. In particular, the program was extended to calculate fluorescence yield from the crystals with multicomponent epitaxial layers[10,14] and from single crystals and crystals with epitaxial films in the Laue case[5] (see Ref. 15 for more references). In the last decade, the program was used to analyze experimental data from a variety of research projects in which the XSW method was applied to interesting physical and material science problems such as the isotopic effect on the lattice constants of Ge[16] and Si[17] (chapter 17), structure of thin HT_c films,[18] polarity of thin GaN,[19] and ferroelectric[20] films (Chapter 16), and others.

In conclusion, the theory and the computer algorithm to calculate secondary radiation yield from the crystal consisting of several layers has been presented. The introduction of multilayer crystals into the XSW method significantly broadened the application areas of this technique. Indeed, in a modern world, a large variety of man-made structures can be considered as layered crystals. These are the homo- and hetero-epitaxial films grown on single crystal substrates (such as semiconductor lasers, photodiodes, and other optoelectronic devices), superlattices, bicrystals, etc. By using the theoretical approach presented in this section and the computer program available nowadays as a free software, the XSW technique in its different modifications can be effectively utilized to perform their structural characterization.

References

1. A. M. Afanasev and V. G. Kohn, *Sov. Phys. JETP* **47** (1978) 154.
2. M. V. Kovalchuk, D. Lil'equist and V. G. Kohn, *Sov. Phys. Solid State* **28** (1986) 1918.
3. M. V. Kovalchuk, V. G. Kohn and E. F. Lobanovich, *Sov. Phys. Solid State* **27** (1985) 2034.
4. J. Zegenhagen, *Surf. Sci. Rep.* **18** (1993) 199.

5. A. Yu. Kazimirov, M. V. Kovalchuk and V. G. Kohn, *Acta Cryst.* A **46** (1990) 649.
6. V. G. Kohn, *Phys. Status Solidi B* **231** (2002) 132.
7. V. G. Kohn and M. V. Kovalchuk, *Phys. Status Solidi A* **64** (1981) 359.
8. M. V. Kovalchuk and V. G. Kohn, *Sov. Phys. Uspehi* **29** (1986) 426.
9. V. G. Kohn, (2007), url: http://kohnvict.narod.ru
10. A. Yu. Kazimirov, M. V. Kovalchuk and V. G. Kohn, *Sov. Tech. Phys. Lett.* **14** (1988) 587.
11. V. N. Schemelev, M. V. Kruglov and V. P. Pronin, *Sov. Phys. Solid State* **12** (1971) 2005–2006; V.N. Schemelev and M.V. Kruglov, *Sov. Phys. Solid State* **14** (1973) 2988–2991; *Sov. Phys. Solid State* **16** (1974) 942–944; *Sov. Phys. Solid State* **17** (1975) 253–256; *So. Phys. Crystallogr.* **20** (1975) 153–157.
12. M. V. Kruglov, E. A. Sozontov, V. N. Schemelevand and B. G. Zaharov, *Sov. Phys. Crystallogr.* **22** (1977) 397–400.
13. M. V. Kruglov, V. N. Schemelev and G. G. Kareva, *Phys. Stat. Sol.* A **46** (1978) 343–350.
14. A. Yu. Kazimirov, M. V. Kovalchuk, A. N. Sosphenov, V. G. Kohn, J. Kub, P. Novak and M. Nerviva, *Acta. Cryst.* B **48** (1992) 577.
15. I. A. Vartanyants and M. V. Kovalchuk, *Rep. Prog. Phys.* **64** (2001) 1009.
16. A. Kazimirov, J. Zegenhagen and M. Cardona, *Science* **28**2 (1998) 930–932.
17. E. Sozontov, L. X. Cao, A. Kazimirov, V. G. Kohn, M. Cardona and J. Zegenhagen, *Phys. Rev. Lett.* **86** (2001) 5329.
18. A. Kazimirov, T. Haage, L. Ortega, A. Stierle, F. Comin and J. Zegenhagen, *Solid State Comm.* **104** (1997) 347–350.
19. A. Kazimirov, G. Scherb, J. Zegenhagen, T.-L. Lee, M. J. Bedzyk, M. K. Kelly, H. Angerer and O. Ambacher, *J. Appl. Phys.* **84** (1998) 1703; A. Kazimirov, N. Faleev, H. Temkin, M. J. Bedzyk, V. Dmitriev and Yu. Melnik, *J. Appl. Phys.* **89** (2001) 6092.
20. M. J. Bedzyk, A. Kazimirov, D. L. Marasco, T.-L. Lee, C. M. Foster, G.-R. Bai, P. F. Lyman and D. T. Keane, *Phys. Rev.* B **61** (2000) R7813; D. L. Marasco, A. Kazimirov, M. J. Bedzyk, T.-L. Lee, S. K. Streiffer, O. Auciello and G.-R. Bai, *Appl. Phys. Lett.* **79** (2001) 515.